J. Fluid Mech. (1987), *vol.* 179, *pp.* 155–177
Printed in Great Britain

Separation and free-streamline flows in a rotating fluid at low Rossby number

By MICHAEL A. PAGE

Department of Mathematics, Monash University, Clayton, Victoria 3168, Australia

(Received 13 May 1986)

The flow past a circular cylinder in a rotating frame is examined when the Rossby number Ro is $O(E^{\frac{1}{3}})$, where E is the Ekman number. Previous studies of the configuration have shown that, provided the ratio $Ro/E^{\frac{1}{3}}$ is less than a certain critical value, the flow around the cylinder is determined by the classical potential-flow solution. However, once $Ro/E^{\frac{1}{3}}$ is greater than that critical value the $E^{\frac{1}{4}}$ layer on the surface of the cylinder, which is rather like a boundary layer in a high-Reynolds-number non-rotating fluid, can separate from the cylinder and distort the potential flow. In this study the form of the flow once separation has occurred is examined using a method analogous to the Kirchhoff free-streamline theory in a non-rotating fluid. The results are compared with published experimental and numerical data on the flow for various values of $Ro/E^{\frac{1}{3}}$.

1. Introduction

In this paper the flow of a rotating fluid of finite depth past an axial circular cylinder will be examined when the Ekman number E is small and the Rossby number Ro is $O(E^{\frac{1}{3}})$. The flow in this configuration has been examined in a number of previous theoretical studies, namely Barcilon (1970), Walker & Stewartson (1972), Merkine & Solan (1979), Page (1985) and Page & Cowley (1987), in two experimental studies by Boyer (1970) and Boyer & Davies (1982), and in a recent numerical study by Matsuura & Yamagata (1985). To date, however, the theoretical studies have been confined to the parameter ranges where the flow is fully attached, thereby considerably restricting the possibility of their comparison with the experimental results, which often show separated flow. In this paper a theory is proposed which aims to describe the flow once separation has occurred and a stagnant region of fluid has formed downstream of the cylinder. This theory includes the important effects due to Ekman suction, but otherwise neglects viscous effects in the main body of the fluid. This can be expected to be an accurate representation provided the Ekman number is sufficiently small so that the $E^{\frac{1}{4}}$ layers occupy only very thin regions of the flow.

As mentioned above, a considerable amount of work has previously been done on the attached-flow problem for flow past a cylinder. For $Ro = O(E^{\frac{1}{3}})$ and $E \ll 1$ the flow can be described in terms of the single parameter $\lambda = Ro/2E^{\frac{1}{3}}$, and Barcilon (1970) demonstrated that for small enough values of λ the motion in the 'interior', which is most of the fluid, is irrotational with the streamlines following the classical potential-flow solution for two-dimensional flow past a cylinder. Close to the cylinder surface there is a thin layer, known as an $E^{\frac{1}{4}}$ layer, across which the flow adjusts to the no-slip condition. It turns out that the flow in this layer can be calculated exactly for $\lambda \ll 1$, and that it has a simple exponential profile with a uniform displacement thickness. For larger values of Ro, so that λ is $O(1)$, the interior flow is unchanged

but the flow in the $E^{\frac{1}{4}}$ layer is governed by a nonlinear equation for which no exact solution is available. At this point Walker & Stewartson appealed to earlier work on the magnetohydrodynamic flow past a cylinder, by Leibovich (1967) and Buckmaster (1969), and concluded that for $\lambda > \frac{1}{4}$ a singularity develops within the $E^{\frac{1}{4}}$ layer at the rear stagnation point. In addition, Buckmaster (1969) was able to show that the flow remains fully attached at this point, and in fact remains attached at least until $\lambda \geqslant \frac{1}{2}$. The precise details of the flow in the $E^{\frac{1}{4}}$ layer between these two critical values were unclear at that stage, although Buckmaster (1971) had made an attempt to describe it, and it was left to Page (1985) and Page & Cowley (1987) to clarify the structure. From the analysis in these studies it is clear that a thin wake forms behind the cylinder for $\frac{1}{4} < \lambda \leqslant \frac{1}{2}$ and that separation occurs once $\lambda > \frac{1}{2}$. The aim of this study is to calculate the flow when $\lambda > \frac{1}{2}$, for which the $E^{\frac{1}{4}}$ layer has separated from the cylinder and distorted the interior flow.

The first step in the calculation of the flow beyond separation is to recognize that in any closed-streamline region, such as the separation bubbles which appear to form in the experiments of Boyer & Davies (1982), the flow is stagnant owing to the exponential decay of vorticity along streamlines, arising through Ekman suction. In addition, the flow outside the separation bubble is irrotational, just as it is for the fully attached flow, and it moves around the bubble as if it were part of the solid obstacle. It then remains to connect these two flow regions together through some sort of relationship to be satisfied on their common boundaries. This situation is similar to that which occurs for high-Reynolds-number flow of a non-rotating fluid past a circular cylinder, and for that case a theory was proposed by Smith (1979) which was based upon the so-called Kirchhoff free-streamline theory. This theory was later modified in Smith (1985) to incorporate a Sadovskii (1971) vortex in the eddy-scale flow, but these modifications do not really affect the structure in this paper since such a vortex will not be found in a rotating flow. As in Smith (1979), the flow under consideration here relies upon the leading-order flow inside the separation bubble being stagnant and on the pressure being continuous across the bounding streamline. In a non-rotating fluid Bernoulli's equation can then be used to deduce that the velocity is constant along the bounding streamline, which in turn enables the position of that streamline to be calculated. The main difference between that situation and the rotating flow is that for the latter there can be no immediate appeal to Bernoulli's equation, owing to the complicating presence of Coriolis forces. Therefore, in this paper an equivalent condition will be derived which enables the free-streamline theory to be extended to these flows, from which the streamline patterns for the inviscid separated flow can be computed.

The plan of the paper is as follows: in §2 the general equations and properties of rotating flows at low Rossby numbers will be outlined, before a perturbation analysis is performed for $E \ll 1$ in §3 to derive the equations for the leading-order velocities in the interior flow. These equations are very similar to the Euler equations for non-rotating flow except for an extra linear 'friction' term which arises through Ekman suction. Then in §4 a modified Bernoulli equation for that flow is derived, enabling a free-streamline theory to be outlined in §5. Some properties of this flow are described in §6, and in §7 the numerical method used to calculate solutions to the proposed problem is outlined. It then remains to examine the results of these calculations in §8 and to compare them with the experimental results of Boyer & Davies (1982) and the numerical results of Matsuura & Yamagata (1985), which are for finite values of the Ekman number E. Finally, some proposals on the form of the more detailed structure, which needs to be considered once higher-order terms in the

flow fields are taken into account, are outlined in §9, based partly on the features of the equivalent non-rotating problem in Smith (1979, 1985).

2. Formulation

Consider a homogeneous viscous fluid, of density ρ^* and constant kinematic viscosity ν^*, which is confined between two infinite parallel plates, a distance d^* apart, and where the entire configuration is rotating with a uniform angular velocity $\Omega^* \hat{\boldsymbol{k}}$ about an axis perpendicular to the plates. Relative to this rotating system, a circular cylinder of radius l^* is placed in the fluid, with its axis parallel to $\hat{\boldsymbol{k}}$, and the fluid is forced past the cylinder by imposing a uniform flow with speed U^* at infinity. Based on these dimensional quantities, three important dimensionless parameters can be defined, namely

$$Ro = \frac{U^*}{\Omega^* l^*}, \quad E = \frac{\nu^*}{\Omega^* d^{*2}}, \quad d = \frac{d^*}{l^*}, \tag{2.1}$$

and these will be referred to as the Rossby number, Ekman number and scaled depth respectively. In this paper, as in Walker & Stewartson (1972) and Page (1982*a*, 1985), both Ro and E are considered to be small, and in particular Ro is taken to be $O(E^{\frac{1}{2}})$. Note, however, that for convenience the definitions of Ro and E used in this paper are slightly different from those in the previous studies. The scaled depth d is assumed to be $O(1)$ with respect to E.

Although the geometry of this configuration is cylindrical, it is generally more convenient to use a Cartesian rather than a polar coordinate system to describe the flow. An exception arises when referring to the cylinder surface, $r = (x^2+y^2)^{\frac{1}{2}} = 1$, but this should usually be clear by the context. The coordinate system is chosen with the z^* axis coincident with the axis of the cylinder and the x^* axis in the direction of the imposed flow at infinity. Dimensionless position and velocity, relative to the rotating frame, can then be defined as $\boldsymbol{x} = (x, y, z) = \boldsymbol{x}^*/l^*$ and $\boldsymbol{u} = (u, v, w) = \boldsymbol{u}^*/U^*$ respectively, where l^* and U^* have been chosen as appropriate length and velocity scales. The fluid is therefore contained in the region with $r > 1$ and $0 < z < d$, and the velocity tends to $\boldsymbol{u} = (1, 0, 0)$ as $r \to \infty$. The equations for a steady flow in these coordinates are

$$Ro(\boldsymbol{u}\cdot\nabla)\boldsymbol{u} + 2(\hat{\boldsymbol{k}} \times \boldsymbol{u}) = -\nabla P + d^2 E \nabla^2 \boldsymbol{u}, \tag{2.2}$$

$$\nabla \cdot \boldsymbol{u} = 0, \tag{2.3}$$

where the dimensional pressure p^* has been scaled to the reduced pressure

$$P = \frac{p^* - \frac{1}{2}\rho^* \Omega^{*2} r^{*2}}{\rho^* U^* \Omega^* l^*}, \tag{2.4}$$

after removing the centrifugal contribution (which does not affect the motion in a closed container). The boundary condition $\boldsymbol{u} = 0$ is applied on all solid surfaces, namely $r = 1$ and $z = 0, d$.

The features of low-Rossby-number, small-Ekman-number flow are now fairly well known; see for example chapter 2 of Roberts & Soward (1978), Walker & Stewartson (1972) or Page (1982*a*, 1985). The main region of the flow is the 'interior' and this is separated from solid boundaries either by Ekman layers, on surfaces which are not parallel to the rotation axis, or by sidewall boundary layers, which occur on surfaces parallel to the rotation axis (such as the cylinder surface). From the Taylor–Proudman theorem, the flow in the interior is, to leading order, both two-dimensional and

geostrophic, so that the leading-order reduced pressure is both constant along streamlines of the flow and independent of the depth z. The Ekman layers, which are within $O(E^{\frac{1}{2}})$ of the surfaces $z = 0$ and $z = d$, are viscous regions which ensure that $\boldsymbol{u} = 0$ on those surfaces. It can be shown that one effect of these layers is to induce a velocity of $O(E^{\frac{1}{2}})$ into, or out of, the interior and this will be seen to induce a frictional effect on the interior flow, through vortex stretching. The sidewall layers, generally known as Stewartson layers when $Ro = 0$, are also viscous regions and they are divided into two parts: a thicker geostrophic layer of thickness $O(E^{\frac{1}{4}})$ which ensures that $u = v = 0$ on the sidewalls; and a thinner ageostrophic layer of thickness $O(E^{\frac{1}{3}})$ which ensures not only that $w = 0$ but also closes the higher-order mass flux in the fluid. This paper will concentrate on the interior flow but will attempt to include the effects of the $E^{\frac{1}{4}}$ layer on that flow, through flow separation off the cylinder and the formation of free shear layers within the interior flow. Unlike the $E^{\frac{1}{4}}$ layers which are attached to a surface, these free shear layers do not enclose an $E^{\frac{1}{3}}$ layer, rather like the $E^{\frac{1}{4}}$ layer in the wake of the flat plate in Page (1983).

3. Governing equations for the interior flow

For Ro of $O(E^{\frac{1}{2}})$ it follows from (2.2) that the leading-order flow $\boldsymbol{u}_0$, for $\boldsymbol{x}$ of order unity, satisfies the geostrophic equation

$$2(\hat{\boldsymbol{k}} \times \boldsymbol{u}_0) = -\nabla P_0, \tag{3.1}$$

where P_0 is independent of z and $w_0 = 0$. Using (3.1) with (2.3), it follows that a stream function ψ_0 can be defined with

$$u_0 = -\frac{\partial \psi_0}{\partial y}, \quad v_0 = \frac{\partial \psi_0}{\partial x}, \tag{3.2}$$

where $\psi_0 = \frac{1}{2}P_0$, but in order to determine ψ_0 it is necessary to examine higher-order terms in (2.2), namely those of order $E^{\frac{1}{2}}$. An equivalent method is to use the same arguments as Page (1982*a*, 1985), introducing the axial component of vorticity $\zeta_0 = \nabla^2 \psi_0$†, and then deriving a vorticity equation from the curl of (2.2).

Since both Ro and the Ekman suction velocity w are $O(E^{\frac{1}{2}})$ it is appropriate to expand all dependent variables in series in powers of $E^{\frac{1}{2}}$, for example

$$P = P_0 + E^{\frac{1}{2}} P_1 + E P_2 + \ldots, \tag{3.3}$$

and to define the parameter $\lambda = Ro/2E^{\frac{1}{2}}$, similar to that used in Page (1982*a*, 1985). Using (2.2) to leading order gives (3.1), and second-order terms give

$$2\lambda \left(u_0 \frac{\partial u_0}{\partial x} + v_0 \frac{\partial u_0}{\partial y} \right) - 2v_1 = -\frac{\partial P_1}{\partial x}, \tag{3.4a}$$

$$2\lambda \left(u_0 \frac{\partial v_0}{\partial x} + v_0 \frac{\partial v_0}{\partial y} \right) + 2u_1 = -\frac{\partial P_1}{\partial y}, \tag{3.4b}$$

$$0 = -\frac{\partial P_1}{\partial z}, \tag{3.4c}$$

with

$$\frac{\partial u_1}{\partial x} + \frac{\partial v_1}{\partial y} + \frac{\partial w_1}{\partial z} = 0 \tag{3.5}$$

† Here and in the remainder of this paper ∇^2 refers to the two-dimensional Laplacian.

from (2.3). From (3.4*c*) it follows that P_1, like P_0, is independent of z and it is then straightforward to show that u_1, v_1 and hence $\partial w_1/\partial z$ are also independent of z. Using the Ekman conditions on $z = 0$ and $z = d$ it follows that

$$\frac{\partial w_1}{\partial z} = -\left(\frac{\partial v_0}{\partial x} - \frac{\partial u_0}{\partial y}\right) \tag{3.6}$$

so that, using (3.5),

$$\frac{\partial}{\partial x}(u_1 - v_0) + \frac{\partial}{\partial y}(v_1 + u_0) = 0. \tag{3.7}$$

It is then possible to define a function ψ_1, which is essentially a stream function for the non-divergent part of the second-order flow, such that

$$u_1 = v_0 - \frac{\partial \psi_1}{\partial y}, \quad v_1 = -u_0 + \frac{\partial \psi_1}{\partial x}, \tag{3.8}$$

and substituting into (3.4*a*, *b*) then gives

$$2\lambda\left(u_0\frac{\partial u_0}{\partial x} + v_0\frac{\partial u_0}{\partial y}\right) + 2u_0 = -\frac{\partial \tilde{P}_1}{\partial x}, \tag{3.9a}$$

$$2\lambda\left(u_0\frac{\partial v_0}{\partial x} + v_0\frac{\partial v_0}{\partial y}\right) + 2v_0 = -\frac{\partial \tilde{P}_1}{\partial y}, \tag{3.9b}$$

where $\tilde{P}_1 = P_1 - 2\psi_1$. Note that these equations now involve only the leading-order velocity components, and they form in effect the momentum equations for those components. Their resemblance to the two-dimensional Euler equations is striking, the only differences being that the parameter 2λ multiplies the advective term and the presence of a linear 'friction' term, due to Ekman-layer effects. Together, (3.2) and (3.9) provide four independent equations in four unknowns (u_0, v_0, ψ_0 and $\tilde{P}_1$) and these can, in principle, be solved in the same manner as might be used to determine the flow of an inviscid non-rotating fluid.

The derivation above is strictly only valid in the interior, where the flow varies on an $O(1)$ lengthscale, but it can be readily generalized to include viscous effects in the $E^{\frac{1}{4}}$ layer, which is also geostrophic. In that case the terms $d^2E^{\frac{1}{2}}\nabla^2 u_0$ and $d^2E^{\frac{1}{2}}\nabla^2 v_0$ appear on the right-hand sides of (3.9*a*) and (3.9*b*), respectively.

4. Modified Bernoulli equation

The governing equations for the interior flow (3.9) can be used to derive a useful condition along the leading-order streamlines, analogous to the Bernoulli equation in an inviscid non-rotating fluid. This condition is, in some sense, a generalization of the constraint derived by Davey (1978) for the circulation around closed streamlines of the flow.

Writing (3.9) in a right-handed coordinate system (s, n), where s is the distance along a streamline measured in the direction of the flow and n is normal to that streamline, implies that

$$\lambda U_0\frac{\partial U_0}{\partial s} + U_0 = -\frac{1}{2}\frac{\partial \tilde{P}_1}{\partial s}, \tag{4.1}$$

with $U_0 = (\boldsymbol{u}\cdot\hat{\boldsymbol{s}})$ as the velocity along the streamline. For a region of the fluid bounded by a closed streamline, on which ψ_0 is constant, (4.1) can be integrated around that streamline to give

$$\oint_{\psi_0=\text{const}} U_0\,\mathrm{d}s = -\tfrac{1}{2}[\lambda U_0^2 + \tilde{P}_1] = 0, \tag{4.2}$$

so the circulation around such a curve is zero. The same is true for all closed curves enclosed within the curve above, and from this it can be deduced that the flow in any closed-streamline region must be irrotational. Since ψ_0 is constant on its boundary, it is then straightforward to show that ψ_0 is constant everywhere within that region, and hence that the flow is stagnant in any region enclosed by a closed streamline. From either (3.9) or (4.1) it is also clear that $\tilde{P}_1$ must be constant in such regions. In §9 it will be become apparent that there is also an $O(E^{\frac{1}{4}})$ contribution to the pressure in the interior, but this will not, in fact, affect these conclusions because that pressure contribution is geostrophic and hence can be lumped with the leading-order term.

As mentioned above, the condition (4.2) is similar to the circulation derived by Davey (1978), and used in both that paper and Page (1982*a*). If §2 were reformulated to allow the lid of the container, at $z = d$, to move with a specified velocity then, after appropriate modification to the Ekman conditions which lead to (3.6), the condition (4.2) is replaced by

$$\oint_{\psi_0=\text{const}} (U_0 - \tfrac{1}{2}U_{\text{lid}})\,\mathrm{d}s = 0, \tag{4.3}$$

where U_{lid} is the component of the lid velocity in the direction of the streamline. This equation is identical with that derived in Davey (1978) using detailed mass-flux arguments. An extension to the case where the base of the container is also in motion is straightforward.

By including the $O(E^{\frac{1}{2}})$ viscous terms in (3.9) it is also possible to derive a form of (4.1) which is valid within the geostrophic $E^{\frac{1}{4}}$ layers. The algebraic details are omitted here, but using the same method as above gives that

$$\lambda U_0 \frac{\partial U_0}{\partial s} + U_0 = -\frac{1}{2}\frac{\partial \tilde{P}_1}{\partial s} - \delta^2 \frac{\partial \zeta_0}{\partial n}, \tag{4.4}$$

where

$$\zeta_0 = \left(\frac{\partial v_0}{\partial x} - \frac{\partial u_0}{\partial y}\right) \tag{4.5}$$

is the leading-order component of vorticity in the $\hat{\boldsymbol{k}}$-direction, and $\delta = d(\frac{1}{2}E^{\frac{1}{2}})^{\frac{1}{2}}$ is the scale thickness of the $E^{\frac{1}{4}}$ layer (similar to that in Page 1982*a*, 1985 after appropriate redefinition of Ro and E). Integrating (4.4) around a stationary solid surface, on which $U_0 = 0$ through the no-slip condition, leads to the constraint

$$\oint_{\psi_0=\text{const}} \frac{\partial \zeta_0}{\partial n}\,\mathrm{d}s = 0, \tag{4.6}$$

which is the equivalent version to (4.2) for the full geostrophic flow, in the sense defined in Page (1982*b*). This condition can be used on such flows in a similar manner to the way in which Davey (1978) and Page (1982*a*) used (4.3), where it removed the non-uniqueness in the solution of Poisson's equation $\nabla^2\psi_0 = \zeta_0$ for a multiply connected region.

As a further sidenote, flows in a container with 'bottom topography', such as those in Page (1982*a*, *b*), have Bernoulli equations identical with (4.1) and (4.4) through

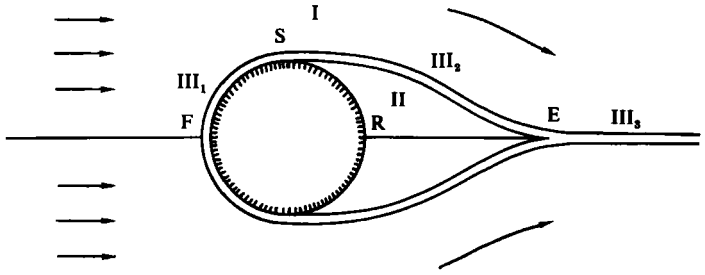

FIGURE 1. Schematic diagram of the leading-order flow regions referred to in §5.

the appropriate modifications to (3.6) and (3.8). This leads to additional terms on the left-hand side of (3.9*a*, *b*) which cancel each other when (4.1) is derived. As a result, most of the theory in this paper can be extended to flows with bottom topography, or equivalently to flows on a β-plane, with little additional effort, although of course such flows will not be irrotational.

5. Free-streamline flows

From (3.9) it can be shown that the leading-order vorticity ζ_0 for the interior flow satisfies the equation

$$\lambda U_0 \frac{\partial \zeta_0}{\partial s} = -\zeta_0 \tag{5.1}$$

along the streamlines $\psi_0 =$ constant. As a result, the vorticity ζ_0 decays exponentially along the streamlines, over a distance of $O(\lambda U_0)$, so that if the flow is uniform far upstream of the obstacle then the vorticity ζ_0 must be zero everywhere in the interior. Exceptions to this arise when a streamline comes close to a solid boundary, where vorticity is generated and then convected and diffused within the $E^{\frac{1}{4}}$ layers. For flow past a circular cylinder Walker & Stewartson (1972) and Page (1985) show, after the slightly different definitions of λ are taken into account, that when λ is less than $\frac{1}{4}$ these $E^{\frac{1}{4}}$ layers remain attached to the cylinder surface and the vorticity is confined to within a distance of $O(\delta)$ from the cylinder. For $\frac{1}{4} < \lambda \leqslant \frac{1}{2}$ the $E^{\frac{1}{4}}$ layers remain attached to the cylinder but a thin wake, also of thickness $O(\delta)$, forms behind the cylinder. In this the vorticity decays exponentially, as would be expected from (5.1) and as also occurs for the wake of a flat plate in Page (1983). Once $\lambda > \frac{1}{2}$ both Walker & Stewartson (1972) and Page (1985) conclude that the $E^{\frac{1}{4}}$ layer separates from the cylinder, rather like the equivalent non-rotating flow at high Reynolds number, and forms a thin free shear layer within the interior flow. It might then be expected, and this is confirmed by the experiments in Boyer & Davies (1982), that these free shear layers enclose a finite region of interior flow; in fact, it will be seen later in this section that they cannot exist freely in this flow without joining each other downstream of the cylinder. As was seen in §4, this implies that the flow in the enclosed region, which is bounded by either the free shear layer or the obstacle, must be stagnant and that both ψ_0 and $\tilde{P}_1$ are constant inside it. The positions of the free shear layers are then determined by ensuring that the modified pressure $\tilde{P}_1$ is constant along them, similar to the requirement on Kirchhoff flows in a non-rotating fluid.

Based on the arguments outlined above, the general features of the interior flow once separation has occurred can be postulated and these are shown schematically

in figure 1. In fact, the flow within region II is rather more complicated than indicated, but this will be readdressed in §9 when higher-order effects are examined. In region I all interior flow streamlines originate from far upstream of the cylinder where the flow is uniform and irrotational, and therefore the flow in the whole of that region satisfies

$$\zeta_0 = \nabla^2 \psi_0 = 0, \tag{5.2}$$

using the arguments outlined in the first paragraph above. From the discussion in §4, or alternatively from (5.1), it is clear that within region II the leading-order stream function ψ_0 is constant, and without loss of generality it can be set to zero. Region III_1 represents the $E^{\frac{1}{4}}$ layer on the surface of the cylinder which separates before the rear stagnation point; as in Smith (1979, 1985), this flow does not encounter a Goldstein-type singularity (Goldstein 1948) at the separation point, but rather leaves the cylinder surface smoothly to form into the free shear layer in region III_2. Since the two free shear layers, one on each side of the cylinder, are aligned with the leading-order flow in region I, they lie along the streamlines of that flow and hence are referred to as free streamlines. The final region shown in figure 1, region III_3, forms the wake of the bubble and, like regions III_1 and III_2, its thickness is $O(\delta)$. Once the positions of the free streamlines are known the effective shape of the obstacle becomes a combination of the forward face of the circle, where region III_1 is still attached, and the stagnant fluid in region II. It is then a straightforward application of potential theory to calculate the interior in region I, although in practice the interrelationship between regions I and II, through region III_2, makes the calculation rather more complicated. Note that region III_3 would not affect this calculation since it has effectively zero thickness and transports no fluid to leading order.

The key to the structure above is the shape of the free streamline. Flows of this form have been examined previously in non-rotating fluids, originating from studies by Helmholtz and Kirchhoff on flow past a flat plate at right angles to an oncoming stream. In that case it is possible to show, based on a different set of equations to (3.9), that the streamwise velocity U_0 is constant along the free streamlines. This, in turn leads to the stagnant region II being infinite in downstream extent, with its width asymptotically proportional to the square root of the distance downstream. Flows of this form were examined further by Brodetsky (1923), Kawaguti (1953), Imai (1953) and Woods (1955), and are described in detail in Thwaites (1960, p. 150). More recently, finite-sized free-streamline flows containing constant-vortex regions have also been the subject of some interest (J. H. B. Smith, 1986) and these are closely related to the flow considered here. It therefore remains to extend such results to a flow in a low-Rossby-number rotating fluid.

The property stated above that U_0 is constant along free streamlines in a non-rotating fluid is a consequence of the leading-order pressure being constant in the separated region, and continuous across the thin shear layers which form the free streamlines. Then, from Bernoulli's equation, the velocity U_0 must also be constant on the outer edge of the free shear layers. For a flow in a rotating frame the latter is not available, and furthermore the leading-order pressure P_0 is already constant on streamlines since $\psi_0 = \frac{1}{2}P_0$. However, the modified Bernoulli equation (4.1) gives further information because $U_0 = 0$ everywhere in region II and therefore $\tilde{P}_1$ is a constant. In addition, it is straightforward to show that, as in a non-rotating flow, the quantity $\tilde{P}_1$ is continuous across the thin shear layers in region III_2. Applying (4.1) again on the outer edge of those layers, it follows that either $U_0 = 0$ or

$$\lambda \frac{\partial U_0}{\partial s} + 1 = 0 \tag{5.3}$$

on the free streamlines, and clearly the latter is most appropriate for that side of the shear layers. This requires that U_0 decrease linearly along the free streamlines, so that

$$U_0(s) = U_0(s_s) - \frac{(s-s_s)}{\lambda}, \tag{5.4}$$

for $s \geqslant s_s$, where s_s is the arclength along the cylinder at which the $E^{\frac{1}{4}}$ layer separates, measured from the forward stagnation point. Note that U_0 must be continuous at s_s, ensuring that the free streamline leaves the cylinder smoothly.

An alternative derivation of (5.4) can be obtained by careful examination of the $E^{\frac{1}{4}}$ layer in region III_2, which separates from the cylinder at s_s. The equations for the flow in this layer are fairly standard, see for example §4 of Page (1982*a*), and in these the right-hand side of the momentum equation has a pressure-gradient-like term of

$$\lambda U_0 \frac{\mathrm{d}U_0}{\mathrm{d}s} + U_0$$

in the current coordinates. Matching with a stagnant flow on one side of the $E^{\frac{1}{4}}$ layer requires that this term be identically zero, and this in turn leads to the condition (5.3) on the flow on the other side. More details of the flow in this shear layer are discussed in §9.

Having determined the condition on the free streamline, it remains to consider whether the flow is now uniquely specified by the boundary conditions on the cylinder, the free streamline and at infinity. In a non-rotating fluid the Kirchhoff free-streamline flow is not unique unless the point of separation s_s is specified in some way, and it is reasonable to expect that the same is true for the problem proposed above (particularly as it will be seen that they are essentially identical when $\lambda \gg 1$). Reviewing the work on the non-rotating problem, Imai (1953) points out that the values of s_s for which a suitable solution exists, with streamlines crossing neither the cylinder nor each other, are between $s_s \approx 0.96$ and $s_s \approx 2.09$. In the absence of viscous effects there is no *a priori* reason to choose any particular one of these values of s_s because all represent solutions of Laplace's equation satisfying all of the requisite boundary conditions. Brodetsky (1923) chose, in effect, $s_s \approx 0.96$, the lower limit of the above range, by assuming that the free streamline has zero curvature at the separation point, but there was no clear reason why that particular condition was appropriate. Kawaguti (1953) reasoned that it was an interaction between the potential flow and the boundary-layer flow which led to separation and so used an iterative approach to see a value of s_s for which both the potential flow and the boundary-layer flow separate at the same point. Using a hodograph method to calculate the potential flow, with a truncated series expansion to represent the conformal mapping, and an approximate integral treatment of the boundary layer flow, he found that the iteration converged once $s_s \approx 1.01$. From this, and it is not clear how, he concluded that $s_s \approx 0.96$ was likely to be the separation point if both the potential and boundary-layer flows were calculated more accurately. It was not until Sychev (1972) used a triple-deck argument to support this assertion that the reason for that particular choice of s_s became apparent. In that paper a self-consistent asymptotic solution was proposed which was able to resolve the singularity in the boundary-layer solution near the separation point, a feat that was not possible under the previous triple-deck proposal by Stewartson (1970). The existence of such a solution was confirmed numerically by Smith (1977) and led to more detailed descriptions of the complete flow in Smith (1979, 1985).

On the basis of the theory in Smith (1977), which applies equally to the

rotating-fluid problem here (Page 1983), the appropriate condition to place on the flow in order to ensure the correct choice of s_s is that not only should U_0 be continuous at s_s, but also $\partial U_0/\partial s$. This in turn ensures that the free streamline has a zero curvature at s_s and also that the tangential pressure gradient along the cylinder $\partial \bar{P}_1/\partial s$ is continuous. Matching the flow against the cylinder for $s < s_s$ with that on the free streamline it follows that

$$\frac{\partial U_0}{\partial s}(s_s^-) = -\frac{1}{\lambda}. \tag{5.5}$$

Having determined the condition (5.4) on the free streamline and the separation condition (5.5), it now remains to solve Laplace's equation and calculate the shape of the stagnant region. In §6 some features of this solution are outlined, prior to solving the problem numerically in §7.

6. Some features of the flow

Many of the detailed features of this flow can be proposed on the basis of the solution to the equivalent non-rotating problem. It is useful to review these, and to obtain some other specialized features, before proceeding to solve the problem numerically because the choice of numerical technique is somewhat dependent upon them.

One feature which is peculiar to the velocity variation given by (5.4) is that an upper bound can be placed on the length of the free streamline. This is possible because $U_0(s)$ must, by definition, be positive along a free streamline and as a result the term $(s-s_s)/\lambda$ in (5.4) cannot exceed $U_0(s_s)$. It is then clear that the length of the free streamline can be no larger than $\lambda U_0(s_s)$ and for a cylinder this would be unlikely to exceed 2λ. An immediate consequence of this is that the free streamlines leaving from either side of the cylinder must meet a finite distance downstream and hence the area of region II must be finite. Also, unless U_0 is identically zero at the reattachment point, and there is no reason why it should be, the two free shear layers will join together in a cusp. This property will become clear once the flow near the reattachment point is examined in detail.

Another feature which might be expected on the basis of the upper-bound 2λ calculated above is that the length of the free streamlines, and hence the size of the stagnant region, increases as λ is increased. As $\lambda \to \infty$ it is reasonable to expect that the stagnant region has a length of $O(\lambda)$ and that U_0 is constant along the free streamlines when viewed on the 'body scale', i.e. an $O(1)$ lengthscale. As a result the flow for $\lambda \gg 1$, when viewed from near the cylinder, is similar to the non-rotating Kirchhoff flow. This feature is discussed further in §9.

Using arguments similar to those in Imai (1953), or otherwise, the form of the stream function ψ_0 can be deduced in the vicinity of the separation point and the strength of the singularity determined. For a flow in which both U_0 and $\partial U_0/\partial s$ are continuous at $s = s_s$ it follows that the radial position of free streamline for $s > s_s$ can be described by a function $r(s)$ with

$$[r(s)-1] \propto (s-s_s)^{\frac{5}{2}} \quad \text{for} \quad (s-s_s) \ll 1. \tag{6.1}$$

The local form of ψ_0 can also be used to show that $U_0(s)$ for $s < s_s$ has the property that

$$\left[U_0(s) - \frac{(s-s_s)}{\lambda}\right] \propto (s_s-s)^{\frac{3}{2}} \quad \text{as} \quad s \to s_s^- \tag{6.2}$$

and hence that $\partial^2 U_0/\partial s^2$ is not finite at the separation point.

Local properties of ψ_0 at the reattachment point, where the free streamlines end, can also be calculated in a similar manner. At that point, where $x = x_e$ and $s = s_e$ say, it is reasonable to expect that U_0 joins continuously onto the flow for $x > x_e$, but there is no reason to suppose that $\partial U_0/\partial s$ will be continuous, or even finite at $x = x_e^+$. To require the latter would, in fact, be overspecifying the problem, and there is no evidence, based on any local analysis of the reattachment point, to suggest that $\partial U_0/\partial s$ should not be discontinuous there. Using arguments similar to those in the previous paragraph, it is clear that the position of the free streamline for $s < s_e$ can be described by a function $y(s)$ with the property

$$y(s) \propto (s_e - s)^{\frac{3}{2}} \quad \text{as} \quad s \to s_e^-. \tag{6.3}$$

The local behaviour of ψ_0 can also be used to show that along the line $y = 0$ for $x > x_e$ the velocity U_0 will increase from its value at reattachment in proportion to $(x - x_e)^{\frac{1}{2}}$ for $(x - x_e) \ll 1$ and eventually tend to $U_0 = 1$ as $x \to \infty$. All of these features are similar to those found at the trailing edge of the eddy-scale flow in Smith (1985), which is based on the constant-vorticity model of Sadovskii (1971).

7. Numerical method

The free-streamline problem arising out of the discussion in §5 is to solve Laplace's equation $\nabla^2\psi_0 = 0$ subject to the boundary conditions $\psi_0 = 0$ on the cylinder surface, $\psi_0 = 0$ and (5.4) on the free streamline, and $\psi_0 \to -y$ as $r \to \infty$, with the supplementary condition (5.5) specifying the separation point s_s. Using the symmetry of the problem about the line $y = 0$, attention can be restricted to the portion of the flow with $y \geqslant 0$ by applying the additional condition $\psi_0 = 0$ on $y = 0$ for $x < -1$ and $x > x_e$, where x_e is the position of the reattachment point.

There are a number of possible techniques which could be used to solve the problem posed above. The first is the hodograph technique, which is the usual method of solving the non-rotating Kirchhoff problem, where the free streamline is mapped conformally on the perimeter of a unit semicircle. This technique is less useful in this case because the free streamlines join behind the cylinder in a singular region which must be treated with some care. A second technique might be to discretize the portion of the cylinder $0 \leqslant s \leqslant s_s$ and also the free streamline $s_s < s \leqslant s_e$, and solve for $U_0(s)$ and $r(s)$ respectively using a boundary-integral method with a radial polar grid. The main difficulty with this proposal is that it is difficult to resolve accurately the form of the free streamline near the singular point at x_e in terms of a function of θ. The method chosen for this paper is, in some sense, a combination of the two methods above; first the region outside the circle is transformed into the upper-half plane using a conformal (Joukowsky) mapping $z' = x' + \mathrm{i}y' = f(x + \mathrm{i}y)$, then a boundary-integral method is used to solve Laplace's equation in the image plane. The inverse transformation $z = x + \mathrm{i}y = g(z')$ can then be used to recover the solution, in the form of an integral, in the original region. This technique removes the need to calculate any quantities other than the transformed shape $y' = Y(x')$ of the free streamline, because the image of the cylinder boundary becomes part of the line of symmetry $y' = 0$ under a Joukowsky transformation.

The particular choice of conformal transformation used in this study is

$$z' = f(z) = \tfrac{1}{2}(x'_l + x'_r) + \tfrac{1}{4}(x'_r - x'_l)\left(z + \frac{1}{z}\right), \tag{7.1}$$

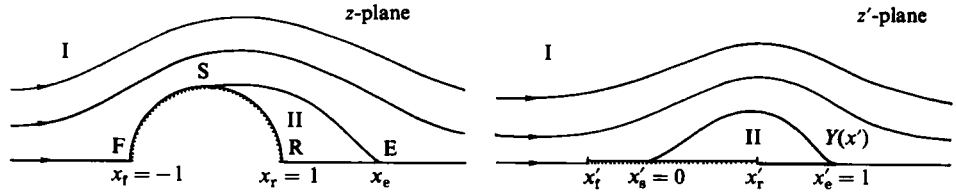

FIGURE 2. Illustration of the region-I flow in both the physical $z = x+iy$ plane and the conformally mapped image plane $z' = x'+iy'$.

where x'_f and x'_r are the images of the forward and rear stagnation points, respectively. The inverse transformation to (7.1) is given by the function

$$z = g(z') = \frac{2}{(x'_r - x'_f)}\{z' - \tfrac{1}{2}(x'_r + x'_f) + [(z'-x'_f)(z'-x'_r)]^{\frac{1}{2}}\}, \tag{7.2}$$

with the branch cut for the square roots chosen to lie on the line $y' = 0$ between x'_f and x'_r. The actual values of x'_f and x'_r are determined by requiring that the separation point s_s map into the origin and the reattachment point x_e map into the point $z' = 1$. As a result the free streamline is mapped into a curve $y' = Y(x')$ for $0 \leqslant x' \leqslant 1$, and the values x'_f and x'_r must lie in the regions $x'_f < 0$ and $0 < x'_r < 1$. All of these features are illustrated in figure 2, where schematic diagrams of both the physical and image planes are shown. For simplicity in later presentation a function $Q(x', y')$ will be defined so that $Q = |\mathrm{d}g/\mathrm{d}z'|$, which is the local magnification factor of the transformation, and Q_∞ will be defined as the value of Q for $r' \gg 1$, i.e. $Q_\infty = 4/(x'_r - x'_f)$.

As a result of the above, the problem to be solved in the transformed plane is to find a solution of $\nabla'^2\psi_0 = 0$ in the image of region I, which satisfies the boundary conditions $\psi_0 = 0$ on $y' = 0$, $\psi_0 \to -Q_\infty y'$ as $r' \to \infty$, with $\psi_0 = 0$ and a transformed version of (5.4) to determine $\partial\psi_0/\partial n'$ on the curve $y' = Y(x')$. In this paper the solution to this problem is written in terms of the boundary integral

$$\psi_0(x', y') = -Q_\infty y' + \frac{1}{2\pi}\int_{s'_s}^{s'_e} \ln\left(\frac{R'_-}{R'_+}\right)\frac{\partial\psi_0}{\partial n'}\,\mathrm{d}s'_1 \tag{7.3}$$

along the free streamline $y'_1 = Y(x'_1)$, where

$$R'_- = [(x'-x'_1)^2 + (y'-y'_1)^2]^{\frac{1}{2}}, \quad R'_+ = [(x'-x'_1)^2 + (y'+y'_1)^2]^{\frac{1}{2}} \tag{7.4}$$

are the distances of the point (x', y') from the points (x'_1, y'_1) and $(x'_1, -y'_1)$, It is convenient to change the variable of integration in (7.3) from s' to x', and use the properties

$$\mathrm{d}n = Q\,\mathrm{d}n', \quad \mathrm{d}s = Q\,\mathrm{d}s', \tag{7.5}$$

so that the equation can be written in the form

$$\psi_0(x', y') = -Q_\infty y' - \frac{1}{2\pi}\int_0^1 \ln\left(\frac{R'_-}{R'_+}\right) U_0 \frac{\mathrm{d}s}{\mathrm{d}x'}\,\mathrm{d}x'_1. \tag{7.6}$$

The quantities in the integrand of (7.6) are then given by

$$U_0(s(x')) = U_0(s_s) - \frac{(s(x') - s_s)}{\lambda}, \tag{7.7}$$

and (5.4), and

$$\frac{\mathrm{d}s}{\mathrm{d}x'}(x') = Q(x', Y(x'))\left[1 + \left(\frac{\mathrm{d}Y}{\mathrm{d}x'}\right)^2\right]^{\frac{1}{2}}. \tag{7.8}$$

The integral (7.6) forms the basis for the numerical method used in this paper but, unlike the usual application of these boundary integrals (as, for example, in Jaswon & Symm 1977), it is not the quantity U_0 that is being sought but rather the position of the boundary curve $Y(x')$. This latter situation is similar to that encountered in some free-surface or bubble problems, for example that in Miksis, Vanden-Broeck & Keller (1981). The major difference between the two types of problem is that solving for U_0 given $Y(x')$ is a linear problem, while seeking $Y(x')$ given U_0 requires that a nonlinear integral equation be solved, and clearly from the form of (7.6), (7.7) and (7.8) the dependence of the integral equation on the shape $Y(x')$ is extremely complicated. While this produces no difficulties in principle, because such nonlinear problems can be solved iteratively using Newton's method, in practice the calculation is algebraically intricate because every quantity in the integrand depends on $Y(x')$ in some way. It is also worthwhile noting at this point that the singularity in the kernel of (7.6), when differentiated with respect to Y, is sufficiently strong to ensure a well-conditioned inversion for $Y(x')$.

To solve (7.6) the range of integration $0 \leqslant x' \leqslant 1$ is the first split into a finite number n of subintervals, with midpoints x_i' for $i = 1, \ldots, n$. Then, given an initial guess for the values of $Y(x_i')$, and the three quantities $U_0(s_s)$, s_s and x_e, the integral can be evaluated using the midpoint rule. The resulting function $\psi_0(x', y')$ is then an approximate solution of Laplace's equation, satisfying the boundary condition on ψ_0 at infinity. To obtain the solution appropriate for this problem it is necessary to place a total of $n+3$ constraints on that integral which, in effect, determine the values of $Y(x_i')$, $U_0(s_s)$, s_s and x_e. These contraints are:

$$\left.\begin{array}{ll} (1, \ldots, n) & \psi_0(x_i', Y(x_i')) = 0, \\ (n+1) & U_0 \text{ continuous at } s_s, \\ (n+2) & \partial U_0/\partial s \text{ continuous at } s_s, \\ (n+3) & U_0 \text{ continuous at } s_e. \end{array}\right\} \tag{7.9}$$

Here the first n conditions ensure that $Y(x')$ is a streamline while the last three are based on properties discussed in §5. To apply the last three constraints on the solution (7.6) requires, in practice, that the integral be differentiated and evaluated at the two points $(x', y') = (0, 0)$ and $(1, 0)$. This is straightforward, since it is only necessary to differentiate the kernel function, and so the details are omitted here.

In this study the simultaneous nonlinear equations which arise from (7.9) were solved using Newton's method, with the derivatives of all quantities evaluated exactly with respect to each of the $n+3$ unknowns. In practice it was found that the error in the iterated quantities did not, in general, converge quadratically to zero as it should; this was probably due to the ill-conditioning in the method with respect to the values of Δs_s and $\Delta Y(x_1')$. Various methods were tried in order to minimize this effect, the most effective of which was to require that $Y(x_2')/Y(x_1')$ be proportional to $(x_2'/x_1')^{\frac{5}{2}}$, in accordance with (6.1), rather than requiring that $\psi_0(x_1', Y(x_1')) = 0$. Another possible difficulty which could arise in this method, but which was not discussed by Miksis *et al*, is that a solution to the discretized nonlinear problem, which is only equivalent to (7.6) in the limit as $n \to \infty$, does not necessarily exist for modest values of n. As a result the errors in the unknown quantities would not converge to zero, but rather would to approach a minimum value which, in turn, would decrease as n is increased. This suggests that perhaps a least-squares approach, with (7.6) evaluated at more than n points, would be a more suitable method for this type of

problem since it would be likely to remove both the difficulties described above. It turned out, however, that the minimum error was within the acceptable limit of $|\Delta Y| < 0.001\, Y_{\max}$ for $n = 50$, so this alternative method was not pursued in this study, although it would probably improve the numerical solutions in any future study.

Since the quantity U_0 in the integrand of (7.6) varies smoothly along the integration curve $y' = Y(x')$, the evaluation of the integral is relatively straightforward. Over each subinterval the singular part of the integrand, arising from the logarithmic kernel, was evaluated exactly using linear interpolation for $Y(x')$ and known integrals. The only quantity appearing in the integral which needed any other type of special treatment was the derivative $\mathrm{d}Y/\mathrm{d}x'$ near $x' = 0$ and $x' = 1$, where the differencing scheme used was modified to take into the account the behaviour of $Y(x')$ from (6.1) and (6.3), viz

$$Y(x') \propto (x')^{\frac{1}{2}} \quad \text{as } x' \to 0^+, \quad Y(x') \propto (1-x')^{\frac{3}{2}} \quad \text{as } x' \to 1^-. \tag{7.10}$$

The method described above is, in fact, quite similar to that used for a constant-vortex flow by Pullin (1984), where a condition equivalent to $Y(x') \propto (x')^{\frac{3}{2}}$ as $x' \to 0^+$ was satisfied at the edge of a flat plate. A more recent study by F. T. Smith (1986) of the Sadovskii (1971) vortex uses a different numerical method and is able to capture such behaviour of the free streamline quite accurately, but unfortunately it requires a large amount of under-relaxation to ensure convergence. The method used in this study converges within the tolerance stated above in five or six iterations.

8. Results and comparison with experiments

In figure 3 the streamlines for the flow past a circular cylinder are shown for four values of $\lambda > \frac{1}{2}$, based on the theory outlined in §5 and using the numerical method described in §7. From these plots it is clear that the length of the stagnant 'bubble' of fluid behind the cylinder increases as λ increases, as was predicted in §6. They also show a pleasing resemblance to both the experiments in Boyer & Davies (1982) and the streamline plots in Matsuura & Yamagata (1985).

For $\lambda = 1$ the region occupied by the stagnant fluid is quite small and confined to the vicinity of the rear stagnation point, where the flow first starts to separate. If λ is reduced from 1 down towards the critical values of $\frac{1}{2}$, the size of the stagnant region decreases smoothly to zero, merging into the attached-flow solution in a regular manner. Undoubtedly a perturbation solution could be calculated for $(\lambda - \frac{1}{2}) \ll 1$, but there does not seem to be much to be gained from that. As λ is increased to 2, shown in figure 3(*b*), the length of the bubble exceeds the cylinder radius and the flow behind the cylinder is beginning to be significantly distorted. It is interesting to notice, however, that the streamlines in front of the cylinder for both $\lambda = 1$ and $\lambda = 2$ are very similar to those for the attached flow. This is no longer the case once $\lambda = 5$ when the stagnant region has roughly the same area as the cylinder and extends more than three radii downstream, although its width does not significantly exceed that of the cylinder. In fact, the shape of the obstacle as a whole is reminiscent of an aerofoil. Once $\lambda = 10$ the stagnant region occupies a large region of the flow and extends about six cylinder radii downstream, and its length appears to be increasing in proportion to λ, a feature which is confirmed in figure 5 (discussed in more detail later). This conforms with the decrease in importance of the 'friction' terms in (3.9), which arise through Ekman suction, as λ is increased so that the flow pattern on the 'body scale' conceivably approaches a form similar to the Kirchhoff

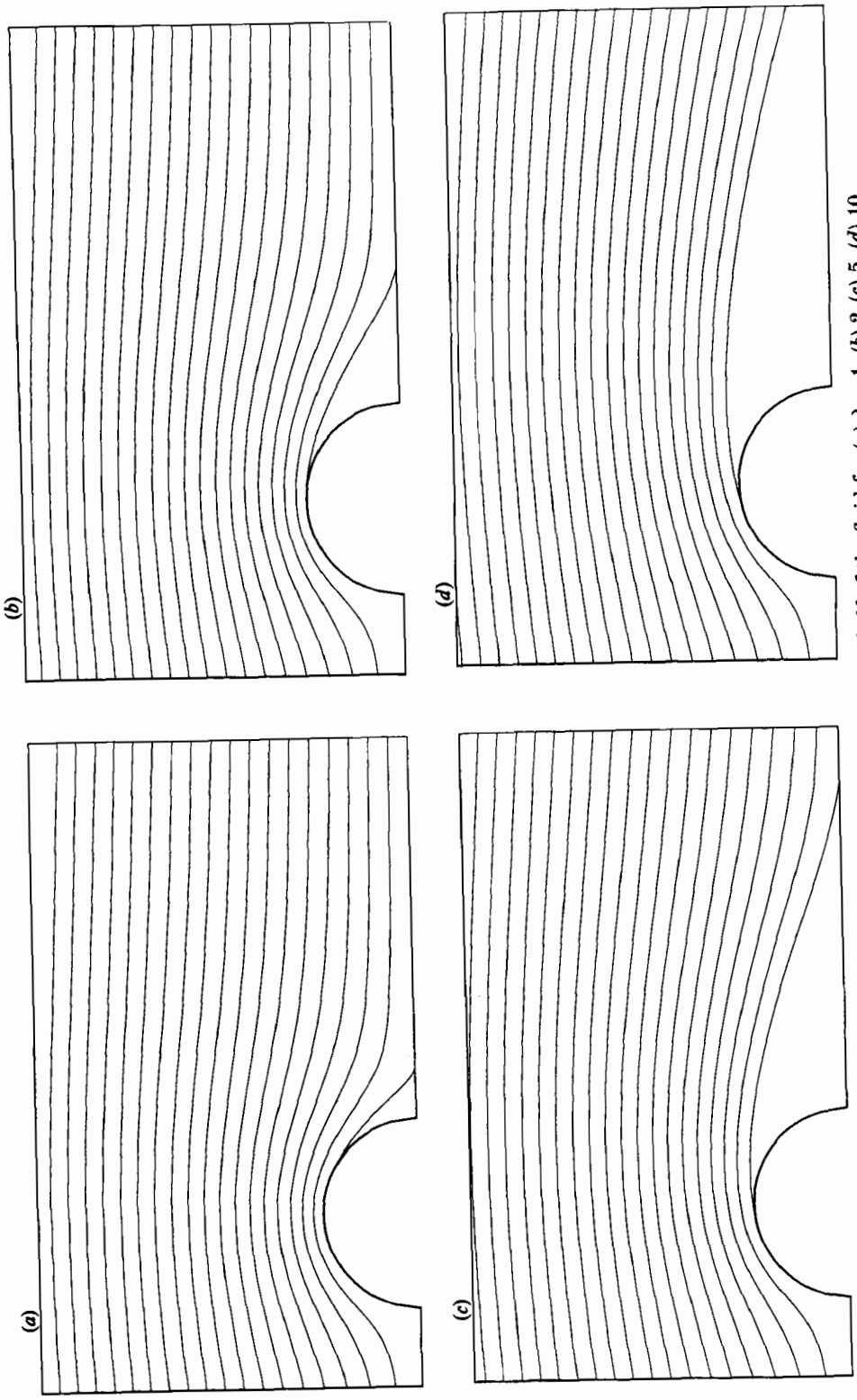

FIGURE 3. Streamline plots of the interior flow in the upper half of the fluid for (*a*) $\lambda = 1$, (*b*) 2, (*c*) 5, (*d*) 10.

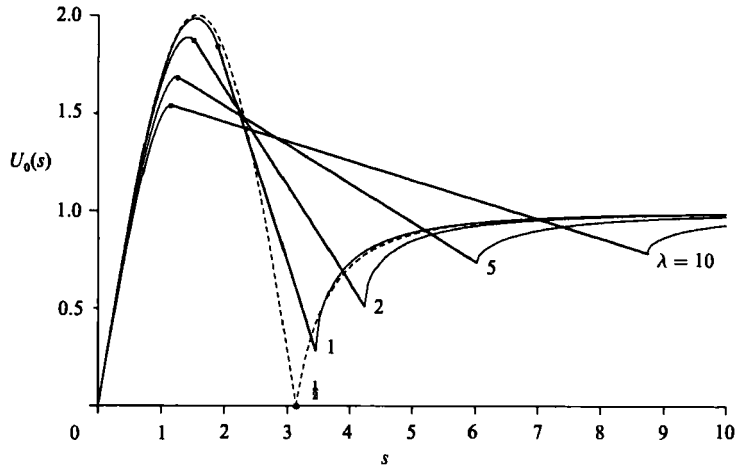

FIGURE 4. Plots of the tangential velocity $U_0(s)$ along the cylinder and on the free streamline for the same values of λ as in figure 3, with an additional curve shown for the flow with $\lambda = \frac{1}{2}$. The separation point s_s is marked with a dot on each curve and the reattachment point s_s is distinguished by the discontinuity in gradient.

solution in a non-rotating flow. This does not mean that the flow for $\lambda \gg 1$ never reattaches; in fact if both spatial coordinates are scaled with λ then it can be expected that the flow of the 'eddy scale' still reattaches in much the same way as it does for smaller values of λ, but that the cylinder reduces in importance when compared to the size of the stagnant region. More details on the flow in this limit are presented in §9.

In figure 4 plots of the tangential velocity U_0 on the streamline $\psi_0 = 0$ are shown for $s \geqslant 0$, which includes the cylinder surface, the free streamline and the wake of the separation bubble. Curves are plotted for the same values of λ as in figure 3, but with $\lambda = \frac{1}{2}$ shown also for comparison. The separation point s_s is marked on each curve and it is apparent that this moves forward monotonically from π as λ is increased from the critical value $\lambda = \frac{1}{2}$. Once $\lambda = 10$ it is already close to the non-rotating value of $s_s \approx 0.96$, which it should approach as $\lambda \to \infty$ on the basis of the remarks in the preceding paragraph. For large values of λ the flow accelerates rapidly around the forward part of the cylinder, reaching a maximum value just before the separation point. The velocity then decreases linearly with s, in accordance with (5.4), until the end of the free streamline is reached. It is also clear from figure 4 that the velocity at the reattachment point, $s = s_e$, increases with λ and is always positive for $\lambda > \frac{1}{2}$. In line with the comments in §6, U_0 increases from $U_0(s_e)$ in proportion to $(s-s_e)^{\frac{1}{2}}$ for $(s-s_e) \ll 1$ and it tends to the free-stream value of $U_0 = 1$ as $s \to \infty$.

Since the configuration being analysed in this paper formed part of the study by Boyer & Davies (1982), namely that with $\beta = 0$, it is possible to compare the numerical results above with the experimental results in their paper. A first impression is that the appropriate photographs look very similar to the plots in figure 3 and have broadly the same properties. Apart from a solely qualitative comparison, which seems to hold up particularly well, a quantitative test on the theoretical results can also be performed using the experimental values for the relative length of the separation bubble, plotted in figures 16, 17 and 18 of their paper. In the conclusions to their study, Boyer & Davies demonstrated that the relative length of the separation bubble increased with their parameters H/R and Ro, and decreased with

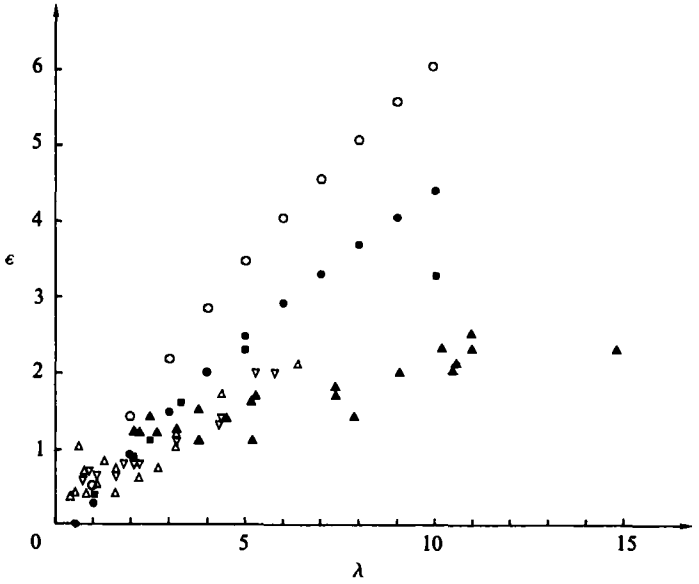

FIGURE 5. Plot of the 'bubble length' ϵ (see text) against λ obtained from the experimental data in Boyer & Davies (1982) for $d = 0.92(\triangle)$; $1.37(\triangledown)$; $2.78(\blacktriangle)$. Also shown (■) are the values calculated in the numerical study by Matsuura & Yamagata (1985) for $\delta^2/\lambda = 0.005$ (their $R_e = 400$); ●, the results of the present study; ○, and the corresponding values of $(x_e - 1)$.

their $Ek = \frac{1}{2}d^2E$. This can be compared with the results of this paper by expressing λ in terms of their parameters, which gives that

$$\lambda = \frac{H}{R}\frac{Ro}{(2Ek)^{\frac{1}{2}}}, \tag{8.1}$$

and observing that this also increases under each of the conditions mentioned above. This is consistent with the trend noted in the first paragraph of this section. The experiments described in their paper were performed for up to eight values of Ro, for four values of Ek and for three values of H/R. As a result they should provide enough data to be able to perform a conclusive comparison with the theory in this paper, which predicts that the bubble length is a function of λ only. To examine this, their 'bubble length' ϵ, defined as the distance from the rear stagnation point to the point at which the half-width of the bubble has decreased to 0.2, is plotted in figure 5 against the values of the parameter λ, using all of the data given in figures 16, 17 and 18 of their paper. A different symbol is used for each value of d, which in practice meant a cylinder of different radius. Despite a considerable scatter in the data, particularly for small values of λ where it is difficult to determine whether or not the flow has separated, there is an apparent increase in ϵ with λ. Such scatter is understandable because in all the experiments the values of δ, the scale thickness of the free shear layer, is non-zero and so it is not easy to determine where the edge of the bubble actually lies. Also shown in figure 5 are the values of ϵ measured from the plots of the inviscid flow in figure 3, showing an approximately linear increase in ϵ with λ, with $\epsilon \approx 0.4\lambda$ for $\lambda \gg 1$. This is rather less than the upper bound 2λ proposed in §6 for the total length of the free streamline.

From the experimental results, it is not particularly clear that a single curve $\epsilon(\lambda)$ can encompass all of the data. Also, once $\lambda > 3$ the experimental values of ϵ seem

to be tending to a limit between 2 and 3 while the theoretical values increase in proportion to λ, thereby exceeding the experimental values by a considerable amount. There are several potential explanations for this, each of which is due to effects neglected in this study. First, for larger values of λ there can still be some residual vorticity in the flow near the cylinder because the vorticity which is unavoidably present at the inflow of the channel decays on a lengthscale of $O(\lambda l^*)$. That some vorticity is remaining in the flow near the cylinder is actually quite clear in many of the photographs. However, the most likely effect of this residual vorticity is to distort the symmetry of the flow rather than significantly affect the length of the bubble. A second possible explanation is due to the presence of the sidewalls of the channel which could restrict the size of the bubble to some extent, although this explanation is not supported by the fact that the results which are most affected are those for the cylinder with the smallest radius (i.e. largest d). Thirdly, and most reasonable, is that the reduction in length could be due to viscous effects in the fluid, such as those considered in §2.4 of Smith (1979) which introduce modifications to the flow of $O(\delta^{\frac{1}{3}})$. Such modifications are equivalent to a displacement of the separation point and relaxing the requirement (6.1) to include an $(s-s_s)^{\frac{3}{2}}$ term that is proportional to $\delta^{\frac{1}{3}}$. Numerical trials in which s_s is moved towards the rear of the cylinder suggest that such an effect can shorten the length of the bubble, but a precise calculation of the modifications requires knowledge of the skin friction at s_s, which will be calculated in a later study of the $E^{\frac{1}{4}}$-layer effects (P. W. Duck & M. A. Page 1987, paper in preparation). In the meantime, it is encouraging to note that the predicted bubble length, shown in figure 5, is least accurate in the experiments with $d = 2.78$. Since these experiments tend to have the largest values of E and hence the largest values of the shear-layer thickness δ, which is proportional to both d and $E^{\frac{1}{4}}$, they will also contain the most significant $O(\delta^{\frac{1}{3}})$ modifications. To illustrate this, typical values of δ calculated for $d = 0.92$, 1.37 and 2.78 are $\delta \approx 0.10$, 0.15 and 0.32, respectively, so clearly viscous effects will be most noticeable in those experiments with $d = 2.78$, which incidentally have the largest values of λ. Furthermore, the eighth power of such values is clearly not small and so it is likely to be able to explain the discrepancies of 50 % apparent in the experimental values of ϵ plotted in figure 5.

Also shown in figure 5 are the numerical results for the bubble length ϵ taken from those presented for $R_e = 400$ in figure 5 of Matsuura & Yamagata (1985). For shorter bubbles these show excellent agreement with the numerical results from this paper, but for $\lambda = 10$ the length is 25 % shorter than that predicted by the inviscid theory. This is, however, in line with the trend in the experimental results noted above, since δ is also largest in that numerical experiment. Although it is not shown here, plotting the numerical results of Matsuura & Yamagata (1985) for smaller values of their R_e, which correspond to larger values of δ, shows a consistent shortening of the bubble as R_e is decreased with λ fixed, further supporting the proposal above that the shortening is due to viscous effects.

Matsuura & Yamagata (1985) also calculate both the drag coefficient of the cylinder and the pressure distribution on the surface, but unfortunately the present theory is unable to predict either of these results. This is because the 'modified pressure' $\bar{P}_1$ includes the contribution to the stream function of order $E^{\frac{1}{2}}$, which cannot be calculated without futher information on the higher-order flow field.

The formal restrictions on the parameters in this study are that $Ro \ll E^{\frac{1}{3}}$, for the same reasons as outlined in Page (1983), that d should be $O(1)$ and that E should be small. In practice, when comparing the theory with experiments, it is usually more appropriate to check the size of $\delta = d(\frac{1}{2}E^{\frac{1}{2}})^{\frac{1}{2}}$, the scale thickness of the $E^{\frac{1}{4}}$ layer, because the theory in this paper relies implicitly upon $\delta \ll 1$.

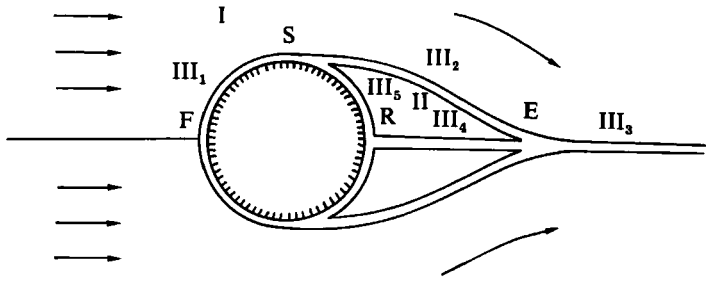

FIGURE 6. Schematic diagram of the higher-order flow regions referred to in §9.

9. Higher-order effects

The stream function shown in figure 3 represents the leading-order flow in only one of the regions described in §5, and so the complete solution to the problem addressed in this paper has not yet been described. To do this it is necessary to consider viscous effects in the fluid, and this leads to the introduction of several other flow regions, additional to those shown in figure 1. A particularly useful guide to the form of these regions comes from the work on the non-rotating problem, and the results in Smith (1979, 1985). Furthermore, those studies, and in particular the second, sound a warning that the solution presented in §§5 and 8 cannot be regarded as the correct limit of the equations as $E \rightarrow 0$ until the higher-order viscous effects have been examined in detail. As in Smith (1985), no attempt will be made here to actually solve for the flow in the higher-order regions, but rather a possible structure will be outlined which the author believes can be reasonably expected to have a self-consistent solution, if not unique.

The structure to be discussed in this section is illustrated in figure 6, and it can be seen that there are two regions, III$_4$ and III$_5$, additional to those shown in figure 1. Also, once viscous effects on the interior flow fields, I and II, are taken into account it soon becomes clear that it is more suitable to expand variables in powers of δ than in powers of $E^{\frac{1}{2}}$, as was done in (3.3). In fact, as Smith (1979) points out, $\delta^{\frac{1}{3}}$ is probably even more appropriate, but this effect will be included within the $O(1)$ flow field, in the manner suggested in that paper. As a result of the $O(\delta)$ corrections above, from this point all terms in the expansions of dependent variables will be referred to by their order with respect to an expansion in powers of δ, so for example u_1 should now be thought of as u_2.

The source of the $O(\delta)$ perturbations to the flow fields is the displacement effect of the viscous $E^{\frac{1}{4}}$ layers in each of the subregions of III, and the consequent mass flux of the same order. First, like the equivalent boundary layer in a non-rotating fluid, region III$_1$ is entraining an $O(\delta)$ flux as it accelerates up the cylinder. This induces a non-zero term ψ_1 in region I, which in turn has a higher-order effect of region III$_1$. Also contributing to ψ_1 in region I are the $O(\delta)$ flux expelled by the free shear layer III$_2$ as the flow decelerates, and the $O(\delta)$ inflow into region III$_3$ as it recovers fluid on its centreline. It is now appropriate to consider what happens near the reattachment point E. As in Smith (1985), part of the velocity profile in region III$_2$ forms into the wake in region III$_3$, and part of it is turned by 180° and proceeds along the line of symmetry in region III$_4$. The turning process is likely to be similar to that shown in figure 2(*b*) of Smith (1985) or figure 4 of Messiter, Hough & Feo (1973), with the lengthscale of the turning region being sufficiently small that viscous and Coriolis forces can be neglected. As a result the portion of the profile with $\psi_1 < 0$ is simply advected around the corner at E. From this starting profile the flow in region III$_4$,

which is really just another $E^{\frac{1}{4}}$ layer, forms a jet along the line $y = 0$ and expells fluid into the interior of region II. This induces a flow of $O(\delta)$ in region II which, according to the results in §5, is stagnant to leading order. As a result there is some flow in region II, albeit small, in the experiments of Boyer & Davies (1982). It is also clear from several of the experiments, for example those shown in figure 19 of their paper, that the jet in region III_4 is carrying fluid from the reattachment point towards the cylinder.

The flow in each of the $E^{\frac{1}{4}}$ layers, making up the various regions III, is governed by a momentum equation of the form

$$\lambda\left(\bar{u}\frac{\partial\bar{u}}{\partial s}+\bar{v}\frac{\partial\bar{u}}{\partial\bar{n}}\right)=\lambda\bar{u}_{\mathrm{e}}\frac{\mathrm{d}\bar{u}_{\mathrm{e}}}{\mathrm{d}s}+\bar{u}_{\mathrm{e}}-\bar{u}+\frac{\partial^2\bar{u}}{\partial\bar{n}^2}, \tag{9.1}$$

where $\bar{v}$ and $\bar{n}$ have been scaled by δ, the direction of n is chosen in a right-handed manner and $\bar{u}_{\mathrm{e}}$ is the flow outside the layer. In particular, in region III_4 the external flow $\bar{u}_{\mathrm{e}}$ is zero and therefore the jet of fluid is continually losing momentum through Ekman 'friction'. Even so, there is no reason to suppose that all of this momentum would have been lost by the time the jet reaches the rear stagnation point R. As a result, a fifth shear layer, labelled III_5 in figure 6, must form on the rear surface of the cylinder, transporting fluid up towards the separation point S. Just as occurred near the reattachment point E, the jet profile would probably turn the corner at R in an inviscid manner. As suggested in Smith (1985), this layer can, in turn, separate before S forming yet another region of interior flow near S. For simplicity this has been omitted from figure 6, and the interested reader is referred to §3.2 of that paper. Ignoring this possibility, the jet would again turn inviscidly at S and become the lower half of the initial profile on III_2, with the upper half having come from region III_1. This profile then proceeds along the free streamline, entraining fluid from region II in the process, until it reaches the reattachment point E and the whose process begins again.

As mentioned in the first paragraph, this structure has not actually been calculated and it will, in fact, form the basis of a later study of the higher-order effects in this configuration (P. W. Duck & M. A. Page 1987, paper in preparation). The crucial test of its suitability is whether a periodic solution exists around the boundary of region II. However, it does seem to close both the $O(1)$ and $O(\delta)$ mass flux, and it is not contrary to either the apparent motion in Boyer & Davies' photographs or the streamline plots in Matsuura & Yamagata (1985).

The next point worth considering is the form of the flow for large values of λ. Based on the results in §8 it is clear that the length of the bubble increases in proportion to λ for $\lambda \gg 1$. The increase in the width is not so clear, but from the form of the Kirchhoff flow it would be expected that the width of the bubble increases in proportion to $\lambda^{\frac{1}{2}}$ in the 'body scale', but decreases proportional to $\lambda^{-\frac{1}{2}}$ relative to the 'eddy scale'. The flow in this limit can probably be calculated using 'slender-body' theory (see for example Thwaites 1960, p. 267) and a limiting form for the shape of the stagnant bubble calculated. This was not attempted in this paper, but will form the basis of a future study by the author. It is worthwhile to contrast the above with the form for the non-rotating flow proposed in Smith (1985); in that case (5.1) is not available to 'remove' vorticity from the eddy, so a wide region of fluid with constant vorticity forms. The flow for a rotating fluid is therefore more like that proposed in Smith (1979) than Smith (1985), but with the extra regions III_4 and III_5. Also, unlike the non-rotating flow, the width of the shear layers and jets remains narrow relative to the cylinder for $\delta \ll 1$. On this point, the reader should note that the $E^{\frac{1}{4}}$ layers

actually have thickness of $O(\delta\lambda^{-\frac{1}{2}})$ for $\lambda \gg 1$ (Barcilon 1970; Page 1983) so for s of order λ, n is still only $O(\delta)$. On the 'body scale', Kirchhoff flow seems to be the most suitable limit and as a consequence the separation point s_s should tend to 0.96 as $\lambda \to \infty$.

10. Conclusions and remarks

Despite the deficiencies noted in §8 when comparing the numerical results with the experiments, the theory described in this paper is able to successfully describe the dominant features of the experiments in Boyer & Davies (1982), particularly when E is small enough that $\delta = d(\frac{1}{2}E^{\frac{1}{2}})^{\frac{1}{2}} \ll 1$. It is unfortunate that the experiments for which that condition is satisfied were limited to relatively small values of λ, but even so there seems to be sufficient support for the theory on the basis of the qualitative comparisons for it to be considered verified. In fact, even if experiments were available for larger values of λ it is quite likely that they would be unsteady, due to a shear-layer instability similar to that in Becker & Page (1987), and hence unsuitable for direct comparison anyway.

By combining the results of this study with those in Walker & Stewartson (1972), Page (1985) and Page & Cowley (1987), a complete description of the flow past a circular cylinder in a rotating fluid can be constructed. This is particularly interesting because by increasing the single parameter λ, with δ asymptotically small, this problem provides a rare example of a flow which starts off as fully attached, with exact solutions available for the flow in both the interior and the boundary layer, through to a flow which develops a singularity within the boundary layer at the rear stagnation point, with a thin wake behind the body, and which further develops into a separated flow, with the separation bubble increasing in length as λ is increased.

One interesting feature of the flow is that the tangential velocity U_0 varies around the cylinder in such a way that the quantity $(\lambda\,\partial U_0/\partial s + 1)$ is positive until immediately before the separation point, and then it becomes zero and remains at precisely that value on the whole of the free streamline. It is interesting to compare this with the necessary condition for separation, originally derived by Buckmaster (1969), which states that separation cannot occur off a solid boundary when the interior flow is such that $(\lambda\,\partial U_0/\partial s + 1)$ is positive everywhere on that boundary. This condition was used by both Page (1982*a*) and Becker & Page (1987) to examine other flows where separation of the $E^{\frac{1}{4}}$ layer can be important and in both those cases fully attached, and apparently self-consistent, $E^{\frac{1}{4}}$-layer flows could be calculated even when $(\lambda\,\partial U_0/\partial s + 1)$ was negative in some parts of the flow. For the flow past a cylinder this seems to be prevented by the development of the singularity at the rear stagnation point (Page 1985; Page & Cowley 1987), which ensures that separation occurs as soon as λ is large enough for $(\lambda\,\partial U_0/\partial s + 1)$ to be zero at that point. For flows in which it can become negative, at the value λ_m say, it would be expected that the flow remains attached until the corresponding $E^{\frac{1}{4}}$-layer flow breaks down with a Goldstein singularity as λ_c say. A 'snap' separation, like that in Stewartson, Smith & Kaups (1982), might then be expected, with λ playing a similar role to the angle of incidence β in that study.

Although these results are outlined for flow past a cylinder, they apply equally to a class of bluff obstacles on which the quantity $\partial U_0/\partial s$ decreases monotonically around the body between the forward and rear stagnation points. For such bodies the criterion for separation would not necessarily be $\lambda > \frac{1}{2}$, but rather it would depend on the value of $\partial U_0/\partial s$ at the rear stagnation point (Buckmaster 1969). For

convenience this paper has concentrated on the flow past a cylinder because of the relatively simple geometry, but all of the results are equally applicable to flows past any obstacle in the above class.

REFERENCES

BARCILON, V. 1970 Some inertial modifications of the linear viscous theory of steady rotating fluid flows. *Phys. Fluids* **13**, 537–544.

BECKER, A. & PAGE, M. A. 1987 Flow separation and unsteadiness in a rotating sliced cylinder. *Geophys. Astrophys. Fluid Dyn.* (to be submitted).

BOYER, D. L. 1970 Flow past a right circular cylinder in a rotating frame. *Trans. ASME* D: *J. Basic Engng* **92**, 430–436.

BOYER, D. L. & DAVIES, P. A. 1982 Flow past a circular cylinder on a beta-plane. *Phil. Trans. R. Soc. Lond.* A **306**, 533–556.

BRODETSKY, S. 1923 Discontinuous fluid motion past circular and elliptic cylinders. *Proc. R. Soc. Lond.* A **102**, 542.

BUCKMASTER, J. 1969 Separation and magnetohydrodynamics. *J. Fluid Mech.* **38**, 481–498.

BUCKMASTER, J. 1971 Boundary-layer structure at a magnetohydrodynamic rear stagnation point. *Q. J. Mech. Appl. Maths* **24**, 373–386.

DAVEY, M. K. 1978 Recycling flow over bottom topography in a rotating annulus. *J. Fluid Mech.* **78**, 497–520.

GOLDSTEIN, S. 1948 On laminar boundary layer flow near the point of separation. *Q. J. Appl. Maths* **1**, 43–69.

IMAI, I. 1953 Discontinuous potential flow as the limiting form of the viscous flow for vanishing viscosity. *J. Phys. Soc. Japan* **8**, 399–402.

JASWON, M. A. & SYMM, G. T. 1977 *Integral Equation Methods in Potential Theory and Elastostatics.* Academic.

KAWAGUTI, M. 1953 Discontinuous flow past a circular cylinder. *J. Phys. Soc. Japan* **8**, 403–406.

LEIBOVICH, S. 1967 Magnetohydrodynamic flow at a rear stagnation point. *J. Fluid Mech.* **92**, 381–392.

MATSUURA, T. & YAMAGATA, T. 1985 A numerical study of a viscous flow past a circular cylinder on an f-plane. *J. Met. Soc. Japan* **63**, 151–166.

MERKINE, L.-O. & SOLAN, A. 1979 The separation of flow past a cylinder in a rotating system. *J. Fluid Mech.* **92**, 381–392.

MESSITER, A. F., HOUGH, G. R. & FEO, A. 1973 Base pressure in laminar supersonic flow. *J. Fluid Mech.* **60**, 605–624.

MIKSIS, M., VANDEN-BROECK, J.-M. & KELLER, J. B. 1981 Axisymmetric bubble or drop in a uniform flow. *J. Fluid Mech.* **108**, 89–100.

PAGE, M. A. 1982*a* Flow separation in a rotating annulus with bottom topography. *J. Fluid Mech.* **123**, 303–313.

PAGE, M. A. 1982*b* A numerical study of detached shear layers in a rotating sliced cylinder. *Geophys. Astrophys. Fluid Dyn.* **22**, 51–69.

PAGE, M. A. 1983 The low Rossby number flow of a rotating fluid past a flat plate. *J. Engng Maths* **17**, 191–202.

PAGE, M. A. 1985 On the low-Rossby-number flow of a rotating fluid past a circular cylinder. *J. Fluid Mech.* **156**, 205–221.

PAGE, M. A. & COWLEY, S. J. 1987 On the flow near the rear stagnation point of a circular cylinder. *J. Fluid Mech.* (submitted).

PULLIN, D. I. 1984 A constant-vorticity Riabouchinsky free-streamline flow. *Q. J. Mech. Appl. Maths* **37**, 619–631.

ROBERTS, P. H. & SOWARD, A. J. 1978 *Rotating Fluids in Geophysics.* Academic.

SADOVSKII, V. S. 1971 Vortex regions in a potential stream with a jump of Bernoulli's constant

at the boundary. *Prikl. Math. Mekh.* **35**, 773–779. (Translated in *P.M.M. Appl. Math. Mech.* **35**, 729–735.)

SMITH, F. T. 1977 The laminar separation of an incompressible fluid streaming past a smooth surface. *Proc. R. Soc. Lond.* A **356**, 443–463.

SMITH, F. T. 1979 Laminar flow of an incompressible fluid past a bluff body: the separation, reattachment, eddy properties and drag. *J. Fluid Mech.* **92**, 171–205.

SMITH, F. T. 1985 A structure for laminar flow past a bluff body at high Reynolds number. *J. Fluid Mech.* **155**, 175–191.

SMITH, F. T. 1986 Concerning inviscid solutions for large-scale separated flows. *J. Engng Maths* **20**, 271–292.

SMITH, J. H. B. 1986 Vortex flows in aerodynamics. *Ann. Rev. Fluid Mech.* **18**, 221–242.

STEWARTSON, K. 1970 Is the singularity at separation removable? *J. Fluid Mech.* **44**, 347–364.

STEWARTSON, K., SMITH, F. T. & KAUPS, K. 1982 Marginal separation. *Stud. Appl. Maths* **67**, 45–61.

SYCHEV, V. V. 1972 Laminar separation. *Izv. Akad. Nauk. SSSR, Mekh. Zh. Gaza.* **3**, 47–59. (Translated in *Fluid Dyn.* **7**, 407–419.)

THWAITES, B. 1960 *Incompressible Aerodynamics.* Oxford University Press.

WALKER, J. D. A. & STEWARTSON, K. 1972 Flow past a circular cylinder in a rotating frame. *Z. angew. Math. Phys.* **23**, 745–752.

WOODS, L. C. 1955 Two-dimensional flow of a compressible fluid past given obstacles within infinite wakes. *Proc. R. Soc. Lond.* A **227**, 367–386.